DEFECT PROOFING TRANSISTOR PACKAGES THROUGH MULTIPHASE-NASTRAN LEADFRAME DESIGN SIMULATOR

Gerry Alvano[1]
Melissa Angelica Camacho[2]
Christopher Cosme[3] and Bongbong Mendoza[3]

Back-end Technology Materials Engineering[1,2,3]
Ampleon Phils. Inc., Binary Street, LISP 1, Brgy. Diezmo, Cabuyao City, Laguna, Philippines 4025
gerry.alvano@ampleon.com, melissa.camacho@ampleon.com, christopher.cosme@ampleon.com, bongbong.mendoza@ampleon.com

ABSTRACT

This study presents a practical, two-pronged integrated approach in eliminating pad top delamination and enhancing mechanical reliability in OMP12XX semiconductor packages. Motivated by a recurring delamination issue in the development of an overmolded package for Industrial, Scientific and Medical use. With the issue being detected through 100% Scanning Confocal Acoustic Tomography (SCAT) inspection after Post Mold Cure (PMC) process, delamination was linked to process-induced oxide formation and insufficient die attach protection, resulting in microscopic interfacial gaps.

Applying the DMADV (Define-Measure-Analyze-Design-Verify) methodology within a six-sigma framework, key process parameters were systematically investigated. Screening DoE, Full factorial DOE to Response Surface Methods revealed that a die bond cure profile with a peak temperature of 250 °C and a cooldown to 40 °C, coupled with a die bond N_2 flow rate of 150 SCFH and a mold leadframe preheat temperature of 125 °C, minimized delamination. Response surface optimization confirmed this parameter set with 100% desirability.

To validate robustness, three production batches of 1,000 units each were manufactured under these optimized conditions. Samples successfully passed JEDEC-level TMCL, uHAST, and HTS tests, while Weibull analysis demonstrated increased characteristic life (η) and improved shape factor (β) at over 90% confidence. To lock-in and integrate as the second prong strategy and meet the target of 98.9% yield, the MSC NASTRAN simulations were conducted to predict and do vibration, thermomechanical, and hygroscopic stress distributions, guiding leadframe design enhancements that reduced peak stresses by up to 40%.

By combining rigorous process optimization with predictive simulation, this work established a scalable, data-driven framework for achieving zero-defect packaging, offering valuable insights for future semiconductor reliability engineering.

1.0 INTRODUCTION

In microelectronic device development, the packaging process critically influences product reliability and electrical performance. Overmolded package architectures are widely adopted due to their compact form factor, high integration density, and favorable electrical characteristics. However, these packages are prone to interfacial delamination at the die pad interface, commonly observed as half-moon delamination. Such defects undermine mechanical integrity which lead to premature electrical failure.

Traditional defect mitigation approaches rely heavily on iterative trial-and-error experimentation, which is often inefficient, resource-intensive, and may fail to identify root causes conclusively. To address these limitations, this study proposes an integrated defect-proofing methodology combining process optimization based on the DMADV framework with simulation-driven design enhancement, using Multiphysics Finite Element Analysis (FEA) with Vibration and Heat Transfer analysis using the NASTRAN platform.

This approach enabled better predictive delamination defects modeling of the material interfaces, including mechanical vibration, moisture absorption, thermal exposure, and thermomechanical stress as the geometry and mesh development can be based on actual leadframe, die and wire bond configurations. Validation was conducted through a dual-track strategy: (1) process optimization focusing on die bond parameter adjustments which narrowed down to nitrogen (N_2) flowrate and cool down temperature change and (2) finite element structural simulations guiding leadframe design improvements to minimize stress concentrations on interfacial parts of the package.

This convergence of experimental process tuning with predictive simulation establishes a robust, scalable framework for defect-proof future of semiconductor package development.

2. 0 REVIEW OF RELATED WORK

Delamination has been acknowledged for an extended period as a frequent reliability concern in semiconductor packaging, typically associated with elements like trapped gases, inadequate adhesion, and thermal discrepancies among materials during manufacturing. Specifically, Lee et al. [1] emphasized that residues from die attach materials if not adequately removed during curing can compromise the interface and cause delamination, particularly following molding. Kondo et al. [2] confirmed this, demonstrating that thermal and humidity stresses can further hasten interfacial deterioration, particularly in regions already compromised by defects from the manufacturing process. One aspect that has attracted interest for managing delamination is the implementation of nitrogen (N_2) in die attach post curing to cooldown process. Research by Huang and Lin [3,4] demonstrated that an appropriate level of nitrogen purge can greatly minimize volatile accumulation, resulting in cleaner bond lines and enhanced adhesion. They also noted that both inadequate and excessive flow rates can be detrimental, either by not effectively removing volatiles or creating uneven thermal conditions that result in additional issues. This emphasizes the significance of meticulous management and enhancement of the nitrogen atmosphere throughout curing.

Beyond this process stage, improvements in simulation have also created new methods to avert defects prior to their emergence. Finite Element Analysis (FEA) tools such as multiphase-NASTRAN are currently utilized not only for failure analysis but also as proactive design instruments. Takahashi et al. [5]. Simulating thermal and mechanical loads in packaging can pinpoint stress hotspots in leadframes and inform design changes like modifying tie bar locations or pad sizes to mitigate failure risks. In a similar manner, Zhang and Chen [6], discovered that alterations in lead geometry guided by simulations greatly enhanced thermal stability and mechanical strength in power transistor packages. Sensitivity to moisture is an additional influencing factor. Smith and Roberts [7] , which created simulation models that monitor the ingress of moisture into the package and the accumulation of internal pressure during reflow or reliability.

3.0 METHODOLOGY

3.1 Process Development Using the DMADV Approach

To address the recurring pad top delamination in OMP12XX packages, the Six Sigma-based DMADV methodology was employed. This structured approach enabled systematic identification, optimization, and validation of critical process parameters contributing to delamination risks.

Define. Initial process mapping and defect documentation were conducted to define the problem scope. Delamination presented as a consistent halfmoon pattern, localized near the short side flanges of the leadframe.

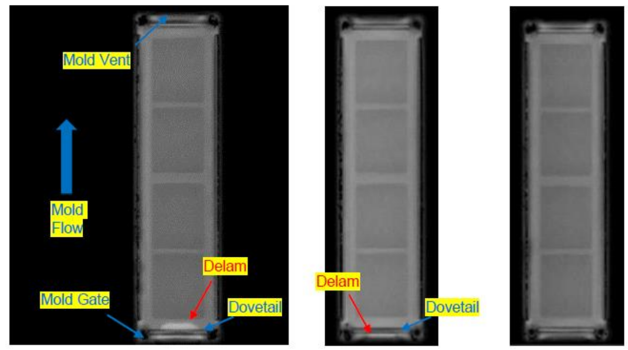

Fig. (1) From left to right (a) SCAT image of inside Dovetail (DA area) (b) SCAT image of outside Dovetail (non-critical area) (c) SCAT image of no Delam.

Strip No.	PD2238001700								PD2238003500							
	U1	U2	U3	U4	U5	U6	U7	U8	U1	U2	U3	U4	U5	U6	U7	U8
Strip 1	D	PD	PD	PD	PD	D	PD	D	D	D	D	D	PD	D	D	
Strip 2	D	PD	PD	PD	PD	PD	PD	D	D	D	PD	D	D	D	D	D
Strip 3	D	D	PD	PD	PD	PD	D		PD	PD	PD	PD	D	PD	PD	D
Strip 4	D	PD	PD	PD	PD	PD	PD	D	D	D	D	D	D	D	D	D
Strip 5	D	D	D	PD	D	D	D		D	D	PD	D	D	D	D	D
Strip 6	D	PD	PD	PD	PD	PD	PD	D	D	D	D	D	D	D	D	
Strip 7	D	PD	PD	PD	D	D	D		D	PD	PD	D	D	D	D	D
Strip 8	D	PD	PD	PD	PD	PD	PD	D	D	D	D	D	D	D	D	
Strip 9	D	PD	PD	D	D	D	D	D	D	PD	PD	PD	D	PD	PD	D
Strip 10	D	PD		PD	PD	PD	PD		D	PD	D	PD	D	PD	D	
Strip 11	D	PD	PD	PD	D		D		PD	PD	PD	PD	PD	D	D	D
Strip 12	D	D	D		D	D	D	D		D	D	D	D	D	D	D
Strip 13					D				D	PD	D	D	D	D	D	D
Strip 14	D	PD	PD	PD	PD	PD	PD	D	D	D	D	D	D	D	D	
Strip 15	D	PD	PD	PD	D	D	D									
Strip 16	D	D	PD	PD	PD	D	D	D								
Strip 17	D	D	D	D	D	D			D	D	PD	D	D	D	D	D
Strip 18	D	PD	PD	PD	PD	PD	PD									
Strip 19	D	D		D	D	D	D	D								
Strip 20	D	D	PD	D	D	D	D									

Legend:	
D	Outside Dovetail (non-critical area)
PD	Inside Dovetail (DA pad area)

Fig 2. Sample Mapping of Delam on Strips

Historical failure analysis (Fig.2) and process mapping through SCAT scan data (example, Fig.1) done after each process step, guided the selection of critical processes for investigation. This identified the half-moon delamination to observed to be present after Post Mold Cure (PMC). No propagation of half-moon pad delamination happens from PMC until singulation and that processes prior PMC were identified potential process contributors for half-moon delamination.

Measure. Historical failure analysis (Fig.2) and process mapping through SCAT scan data (example, Fig.1) done after each process step, guided the selection of critical processes for investigation. This identified half-moon delamination is observed after PMC. No processes prior PMC were identified potential process contributors for half-moon delamination., Quantitative data was gathered through Ishikawa diagram shared in Appendix A, which narrowed down the root cause to High DA_CD Temp and LF design (limited relief holes).

Experiments, covering (1) Die bond N_2 Flowrate with setpoints at 0, 5, 7, and 10 SCFH. (2) LF Preheat Time: Intervals at 0, 3, 5, and 10 seconds. And (3) Leadframe Surface State: Plasma-cleaned vs. uncleaned followed with responses covering the adhesion strength via die shear testing, delamination frequency via SAT (Scanning Acoustic Tomography), residual content via TGA (Thermogravimetric Analysis), surface characterization via SEM and EDX and oxide thickness via XPS (X-ray Photoelectron Spectroscopy)

Analyze

Failure modes were correlated with process parameters using statistical analysis and theoretical principles:
Arrhenius Law for epoxy cure kinetics are utilized:

$$k = A \cdot e^{-\frac{E_a}{RT}} \quad \text{(Eq.1)}$$

where k is the cure rate constant.
Surface energy and wetting theory (Young's equation):

$$\gamma_{SV} = \gamma_{SL} + \gamma_{LV} \cdot \cos\theta \quad \text{(Eq.2)}$$

Diffusion theory (Fick's Law) to understand moisture effects. First-order degradation kinetics to interpret TGA weight loss curves:

$$\frac{dW}{dt} = -kW \quad \text{(Eq.3)}$$

Process interaction effects were evaluated using Minitab's response surface model and validated through SAT cross-sections and post-mold curing (PMC) evaluation.

Design and Verify

Optimized parameters were established: 6 SCFH N_2 flowrate, 3-second LF preheat, dual N_2 zone activation, and plasma-treated leadframes. These were implemented in full process runs and verified through reliability tests such as High Temperature Storage (HTS) at 150°C for 1000 hours, uHAST at 160°C/85%RH for 96 hours, Weibull lifetime projections and confidence interval analysis

3.2. Development of NASTRAN-Based Mechanical Simulation for Design Validation

To complement process improvements and enable predictive failure avoidance, a Finite Element Method (FEM) simulation framework was developed using MSC NASTRAN, focusing on vibration, thermomechanical, and moisture-induced stress across a two-week end-to-end processing cycle.

Geometry and Meshing

The 3D model of the SOT leadframe and mold compound was developed in CAD and imported into MSC NASTRAN. High-resolution meshing was applied at critical regions such as the tie bars, die paddle corners, and flange areas where stress concentrations were previously observed.

Vibration Simulation

Modal and Harmonic Response analyses were performed to assess resonant behavior and forced vibrations, simulating handling-induced excitation.
Governing equation:

$$[M]\{\ddot{u}\} + [C]\{\dot{u}\} + [K]\{u\} = \{F(t)\} \quad \text{(Eq.4)}$$

where [M], [C], and [K] represent the mass, damping, and stiffness matrices, respectively.

Critical modes were compared to real-world vibration spectra to identify high-risk conditions. Design iterations added tie bars and curvature to high-strain locations to detune frequencies and minimize peak strain.

Thermomechanical Simulation

Static Structural and Nonlinear Static analyses modeled stress from Coefficient of Thermal Expansion (CTE) mismatch during reflow and post-mold curing. Stress development followed the thermoelastic stress equation:

$$\sigma = E \cdot \Delta\alpha \cdot \Delta T \quad \text{(Eq.5)}$$

where E is Young's modulus, $\Delta\alpha$ is the differential CTE, and ΔT is the temperature change. Material properties (CTE, modulus, Poisson's ratio) were calibrated from actual datasheets and DPC-measured values.

Hygroscopic Swelling Simulation

Moisture uptake and its mechanical impact were simulated using coupled diffusion-structural analysis, with input from 85% RH conditions for 2 weeks, based on the MSL3 exposure profile.

Fick's Second Law governed diffusion were also simulated to obtain the hygroscopic strain:

$$\frac{\partial C}{\partial t} = D\frac{\partial^2 C}{\partial x^2} \quad \text{(Eq.6)}$$

Hygroscopic strain calculated by:

$$\varepsilon_h = \beta \cdot C(t) \quad \text{(Eq.7)}$$

where β is the moisture expansion coefficient and C(t) is moisture concentration. Moisture-induced stress distributions were mapped and compared with known delamination-prone areas.

Model Validation

Simulated outputs were validated against physical package builds subjected to:

- Thermal cycling (–40°C to 150°C, 1000 cycles)
- JEDEC MSL3 exposure and reflow
- Post-stress SAT inspection and cross-sectional FA

Strain and stress hotspots predicted by NASTRAN were aligned with prior failure cases, affirming the model's predictive accuracy.

4.0 RESULTS AND DISCUSSION

4.1 DMADV-Driven Resolution of Halfmoon Delamination in OMP12XX Packages

To systematically address the recurrent half-moon delamination observed in OMP12XX packages, the DMADV (Define–Measure–Analyze–Design–Verify) methodology was implemented, adhering to the Six Sigma design framework to achieve robust and statistically validated process improvements. Comprehensive process mapping identified that half-moon delamination was consistently detected through SCAT inspections following PMC (with 100% SCAT conducted post-PMC during qualification), without evidence of propagation from PMC to singulation. Furthermore, upstream processes prior to PMC were recognized as potential contributors to the initiation of half-moon delamination, warranting targeted investigation and optimization.

Samples from this process mapping are decapped which indicated a build-up of oxides that is localized to the gate side post PMC. Validating with unmolded samples run in parallel, initial increase in Cu oxide formation was initially seen at post die attach area. Thus , it is hypothesized that due to the high heat temperature and high heat flow concentration on this area, exposure of leadframes starting from the die attach cure oven with elevated temperature and high O2 concentration could have build the high oxide concentration areas observed on decapped molded samples post PMC.

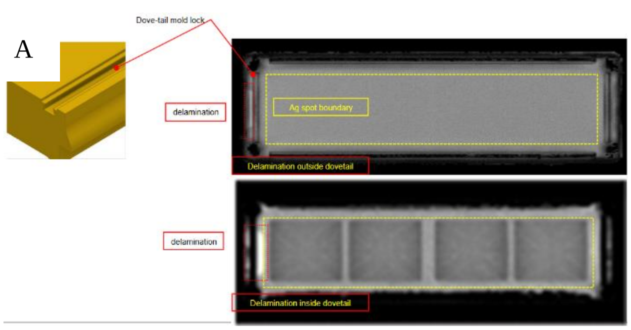

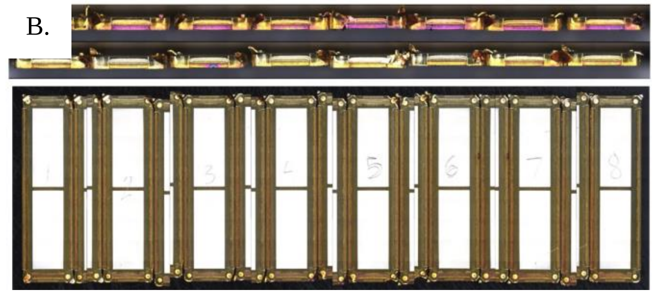

Fig 3. Images of (A) SCAT image of delamination observed post PMC (B) mechanically decapsulated samples showing flange area discoloration indicative of oxidation.

This pointed to the root cause analysis (Appendix A) results, which narrowed down to High DA_CD Temp and LF design (limited relief holes). To validate the interaction of die bond cure temp, die bond N2 flowrate and mold leadframe preheat time, a screening DOE was made. Fig.4 shows the screening DOE results which narrowed down the significant factors to die bond N2 flowrate, where N2 flowrate is better than low flowrate. At mold LF preheat time, that the shorter leadframe preheat time is better than longer time and that the interaction of the N2 flowrate and the low LF preheat time showed better response.

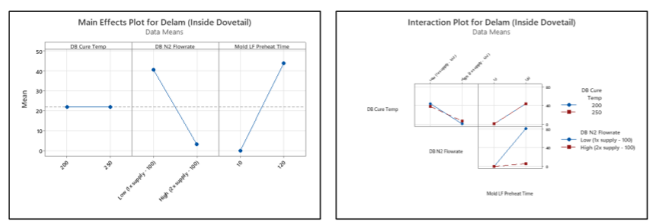

Factor Information

Factor	Levels	Values
DB Cure Temp	2	200, 250
DB N2 Flowrate	2	Low (1x supply - 100), High (2x supply - 100)
Mold LF Preheat Time	2	10, 120

Model Summary

S	R-sq	R-sq(adj)	R-sq(pred)
6.25	99.19%	97.15%	86.99%

Analysis of Variance

Source	DF	Adj SS	Adj MS	F-Value	P-Value
Model	5	9531.25	1906.25	48.80	0.020
Linear	3	6640.62	2213.54	56.67	0.017
DB Cure Temp	1	0.00	0.00	0.00	1.000
DB N2 Flowrate	1	2812.50	2812.50	72.00	0.014
Mold LF Preheat Time	1	3828.12	3828.12	98.00	0.010
2-Way Interactions	2	2890.62	1445.31	37.00	0.026
DB Cure Temp*DB N2 Flowrate	1	78.13	78.13	2.00	0.293
DB N2 Flowrate*Mold LF Preheat Time	1	2812.50	2812.50	72.00	0.014
Error	2	78.13	39.06		
Total	7	9609.37			

Fig 4. Screening DoE DB cure temp, DB N2 flowrate and Mold LF preheat time.

To identify and refine the critical parameters influencing overall pad delamination, a full factorial design of experiments (DOE) with an increased sample size was performed. As illustrated in Fig. 5, Pattern 2, utilizing a lower cooldown temperature of 40 °C, exhibited improved delamination performance compared to Pattern 9, which employed an 80 °C cooldown. Additionally, a die bond N_2 flow rate of 150 SCFH demonstrated superior performance relative to 100 SCFH. While a higher mold leadframe preheat temperature generally reduced delamination, it was observed to exacerbate delamination when combined with the lower N_2 flow rate of 100 scfh.

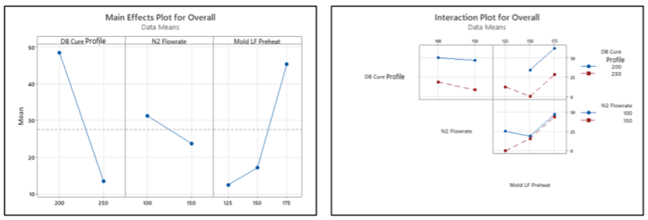

Factor Information

Factor	Levels	Values
DB Cure Profile	2	200, 250
N2 Flowrate	2	100, 150
Mold LF Preheat	3	125, 150, 175

Model Summary

S	R-sq	R-sq(adj)	R-sq(pred)
2.55155	99.60%	98.79%	*

Analysis of Variance

Source	DF	Adj SS	Adj MS	F-Value	P-Value
Model	6	4839.84	806.64	123.90	0.001
Linear	4	4751.95	1187.99	182.48	0.001
DB Cure Profile	1	2363.28	2363.28	363.00	0.000
N2 Flowrate	1	244.14	244.14	37.50	0.009
Mold LF Preheat	2	1585.29	792.64	121.75	0.001
2-Way Interactions	2	191.41	95.70	14.70	0.028
N2 Flowrate*Mold LF Preheat	2	191.41	95.70	14.70	0.028
Error	3	19.53	6.51		
Total	9	4859.37			

Fig 5. Full factorial DOE results , showing the interaction of die bond cure profile, N2 flowrate and Mold LF Preheat.

To confirm the results surface characterization was also done in parallel. The OMP12XX leadframe revealed oxidation and carbon contamination sensitivity. Oxidation in pattern 9 condition leads to non-uniform Cu oxide growth, increasing interfacial energy and reducing adhesion. These effects correlate with the Smith [6] ‘s approach to adhesion, which relates lower surface energy to reduced wetting and bonding performance.

To remove other factors that could affect this interaction. A verification of the effectivity of plasma cleaning using Ar+H_2 was also made. This is done to check the effectivity of removing oxides and how this could help increase the adhesion post die attach process as it is known that plasma cleaning contributes to lowering surface energy and improving bond uniformity.

Comparison of the oxides concentration and roughness values showed rougher topography near rivets and dovetails, however, initial validation done by the team showed no statistically significant difference on oxides concentrations before and after plasma cleaning. Revalidation of this initial results indicated that, this difference may not have reached significance due to limited sample size, emphasizing the need to add this in the screening DOE trials.

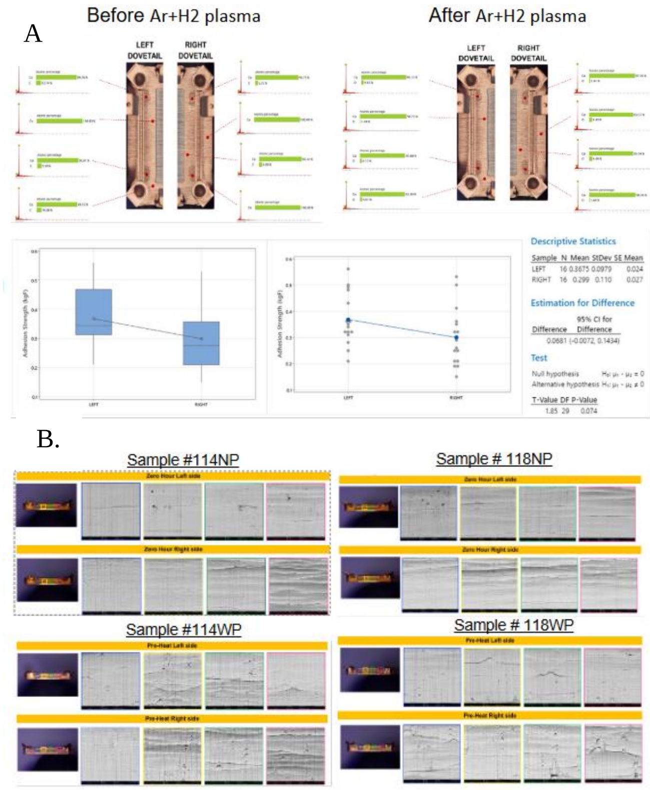

Fig 6. Characterization of (A) flange sidewalls and (B) de-capped mold to validate the potential sources of variation.

Returning to the response surface analysis, Fig. 7 presents the response optimizer results, which identified with 100% desirability the optimal parameter combination: a die bond cure profile corresponding to Pattern 2 (250 °C peak temperature with a 40 °C cooldown), a die bond cure N_2 flow rate of 150 scfh, and a mold leadframe preheat temperature of 125 °C.

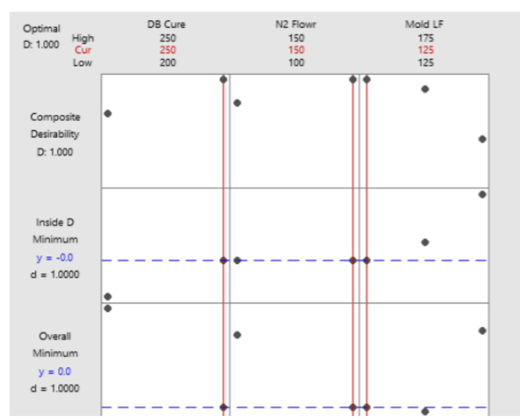

Fig 7. Response optimizer results.

To ensure consistency of results, three batches of leadframes comprising 1,000 units each were processed. Samples from these batches underwent reliability testing and successfully passed JEDEC-level requirements, including TMCL, uHAST, and HTS evaluations. Subsequent Weibull analysis demonstrated increases in both characteristic life (η) and shape parameter (β), with confidence levels exceeding 90%, thereby supporting the robustness of the proposed model.

$$F(t) = 1 - e^{-\left(\frac{t}{\eta}\right)^{\beta}} \qquad \text{(Eq. 8)}$$

where higher β indicates lower variability and stronger reliability.

4.2 NASTRAN-Based Simulation for Mechanical Reliability Validation

To validate the design related concern on leadframe hotspot that contributed to the halfmoon delamination in this area, simulation framework was developed in MSC NASTRAN to predict mechanical failure mechanisms in OMP12XX-based packages, addressing vibration, thermomechanical, and hygroscopic effects during a typical 2-week processing and shipping cycle. The objective was to proactively validate leadframe and die pad geometries using leadframe models grounded in solid mechanics and heat/mass transfer theory.
Vibration simulations and harmonic response analyses focused on resonance and forced response of leads and paddle structures. Governing equations included:

$$[M]\{\ddot{u}\} + [C]\{\dot{u}\} + [K]\{u\} = \{F(t)\}$$

where [M], [C], and [K] are the mass, damping, and stiffness matrices, respectively. Natural frequencies between 210–270 Hz overlapped with factory handling conditions. Redesign with tie bars and curved transitions redistributed stress and reduced peak strain from >5% to <2%, detuning the design from harmful excitation frequencies.

Vibration Simulation

Design changes including adjustment in vent position and area, change the mass distribution, total surface area and center of gravity of the package. These changes affect how the package responds to vibration in real-world conditions. Vibrational simulation results with direct frequency response of 3 Hz to 100 Hz, as shown in Fig 8 showed that even with small changes, like adding or moving vent holes, could double the lead frames maximum vibration displacement. This highlights the importance of considering mass and geometric shifts during design tweaks.

A)

B)

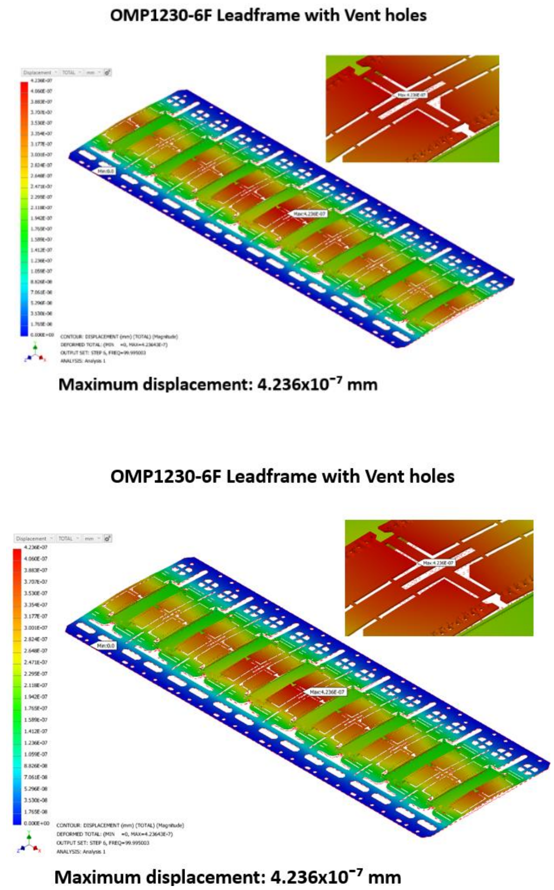

Fig.8 Vibrational Analysis simulated using Nastran Fusion showing direct frequency response for leadframes without vent holes (A) and leadframes with vent holes for a 3Hz-100Hz applied frequency.

Thermomechanical Simulation

High stresses were identified at the mold-to-die interface and lead transitions. Comparing the simulations done to validate the die stress compared with die attach interface stress Fig. 9. Simulation results showed geometry adjustments indeed reduced stress accumulation by up to 40%, in agreement with empirical reliability data.

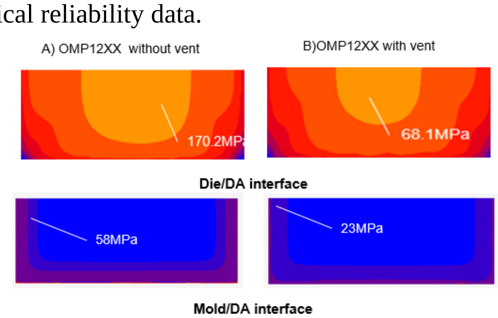

Fig.9 Thermomechanical stress simulation at the die-to-die attach interphase and mold-to-die attach interphase.

Hygroscopic Swelling Simulation

Moisture ingress and hygroscopic swelling modeled using Fick's Second Law and coupled structural-moisture analysis showed that strains introduced shear stress at die-to- mold-to lead frame interface.

Final builds validated through JEDEC MSL3 thermal cycling and SAT showed no delamination or voiding, confirming model accuracy. Simulation-predicted failure zones correlated with prior failure analysis locations, validating the FEM approach as an effective predictor of package integrity.

The combined application of DMADV methodology and NASTRAN-based multiphysics simulation provided a robust and holistic understanding of the failure and the framework necessary in resolving half-moon delamination. Process-driven improvements targeted root causes using chemical kinetics, adhesion theory, and surface science, and DMADV with simulation integrated structural dynamics, thermomechanics, and mass diffusion principles guided the design decisions. This holistic integration establishes a predictive, zero-defect paradigm for advanced semiconductor packaging.

5.0 CONCLUSION

This study successfully demonstrated a dual-pronged strategy for defect-proofing semiconductor packages by combining data-driven process optimization through the DMADV methodology with predictive design validation using MSC NASTRAN finite element simulations.

For the OMP12XX ISM packages, the primary defect of pad top (half-moon) delamination was resolved by identifying and the optimizing key process parameters specifically, the die bond cure profile, the die bond cure N_2 flow rate of 150 SCFH, and a mold leadframe preheat temperature of 125 °C.

Using MSC NASTRAN-based simulations provided a theoretical and quantitative basis for redesigning the leadframe geometry to mitigate thermomechanical stresses encountered during process-induced heating, cooling, and environmental exposure. The simulated plastic strain distribution, derived from thermal-mechanical equations and material properties, guided structural enhancements including tie bar reinforcement and die paddle smoothing, reduced the maximum strain levels in this area of the leadframe. Experimental thermal cycling validated these enhancements with zero observed delamination.

The integration of these approaches established a scalable, predictive, and defect-eliminating framework for semiconductor packaging, significantly improving both process reliability and mechanical integrity of the next generation of over-molded packages developed.

6.0 RECOMMENDATIONS

Based on the findings and successful outcomes of this study, the following recommendations are proposed to ensure sustained defect prevention and continuous improvement in semiconductor packaging processes and design validation:

1. Incorporate MSC NASTRAN or equivalent simulation tools during the early design stage of new leadframe-based packages. Modal, thermal, and hygroscopic simulations should be used to forecast failure-prone regions and inform geometry improvements before physical prototyping.
2. Implement a cross-functional development approach, ensuring active collaboration among design, process, and reliability engineering teams to unify theoretical models with practical experimentation.
3. Extend the simulation scope to include multiphysics modeling, incorporating moisture diffusion, CTE mismatch, and vibration fatigue to predict long-term degradation effects across extended supply chain exposures.

This integrated methodology not only resolves existing packaging defects but also builds a foundation for sustainable, first-pass-yield success in high-reliability semiconductor products.

7.0 ACKNOWLEDGMENT

The authors would like to thank the following for their support in this study:

- – Sr. Materials Engineer BET R&D Ampleon Phils., Inc.
- Donald Locana – Senior Manager / NPI-BET Quality, Ampleon Phils., Inc.
- Marilou Bigcas – Senior Director, Assembly Process, Factory General Management, Ampleon Phils., Inc.
- Nenita Ignacio – Senior Manager, Supplier Quality and IQC, Global Quality Management, Ampleon Phils., Inc.

8.0 REFERENCES

1. Lee, S., Kim, J., & Park, H. (2020). *Influence of Die Attach Outgassing on Delamination in Semiconductor Packaging*. Journal of Electronic Materials, 49(7), 4321–4330. https://doi.org/10.1007/s11664-020-08345-x

2. Kondo, T., Tanaka, M., & Saito, Y. (2021). *Thermomechanical Reliability of Overmolded Packages under High Humidity Stress*. Microelectronics Reliability, 121, 114135. https://doi.org/10.1016/j.microrel.2021.114135
3. Takahashi, K., Nakajima, H., & Watanabe, T. (2019). *Structural Optimization of Leadframes Using Multiphase-NASTRAN Simulation to Prevent Thermomechanical Failures*. IEEE Transactions on Components, Packaging and Manufacturing Technology, 9(3), 587–594. https://doi.org/10.1109/TCPMT.2019.2892320
4. Huang, Y., & Lin, W. (2018). *Effect of Nitrogen Purge Flow on Die Attach Cure and Delamination in Molded Semiconductor Packages*. Journal of Electronic Packaging, 140(2), 021004. https://doi.org/10.1115/1.4038750
5. Zhang, L., & Chen, D. (2017). *Finite Element Analysis for Thermal Stress Reduction in Leadframe Design of Power Transistor Packages*. Microelectronics Journal, 64, 60–68. https://doi.org/10.1016/j.mejo.2017.01.012
6. Smith, J., & Roberts, P. (2016). *Modeling Moisture-Induced Delamination in Plastic Encapsulated Microcircuits*. IEEE Transactions on Device and Materials Reliability, 16(1), 23–30. https://doi.org/10.1109/TDMR.2015.2496540

9.0 ABOUT THE AUTHORS

Gerardo A. Alvano is a graduate of BS Mechanical Engineering at the Technological Institute of the Philippines. A Mechanical Designer for the past 20 years. He is currently under the Quality and Materials Engineering Group. Gerry is directly involved in early Package development programs, generating digital prototypes, helping in tooling design study, checking adaptability to current manufacturing set-up, and ensuring products conformance to quality.

Melissa Angelica C. Camacho currently works as a Principal Materials Engineer, leading the Materials Competence Center - R&D at Ampleon Inc. In this capacity, she drives research and development initiatives centered on materials characterization, selection, and innovation for advanced RF power semiconductor packages, including design reviews for LDMOS and GaN devices. Her expertise encompasses leadframes, die attach materials, molding compounds, and interconnection technologies, with a strong emphasis on plasma surface processes and thin film applications.

Cristopher Cosme Cristopher A. Cosme is currently a Principal Wirebond Process Development Engineer at Ampleon Inc., where he leads the Wirebond Competence Center – R&D. He has over 23 years of experience in the semiconductor industry, specializing in wire bonding processes, including wedge bonding for aluminum and gold wires, as well as ball bonding for gold and copper wires.

Bongbong A. Mendoza is a Principal Engineer and Project Manager for Back End Technologies (R&D) at Ampleon, with over 30 years of experience in the semiconductor industry. He began his career in SMT and Die Attach and has since led the successful release of multiple GaN packages for RF power applications.

10.0 APPENDIX

Appendix A. Ishikawa Diagram- Halfmoon Delamination

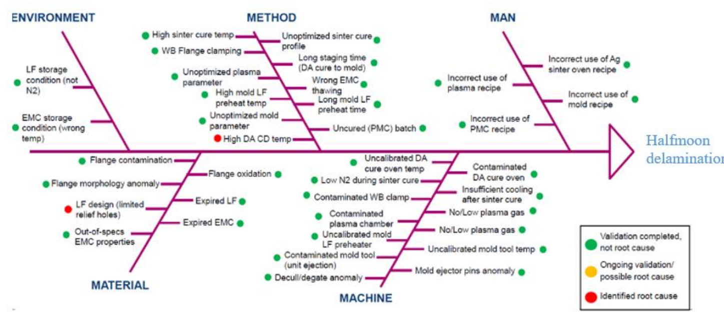

.

Appendix B

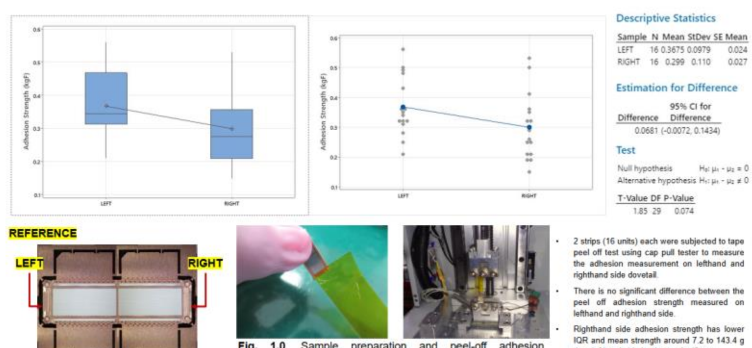

Fig. 1.0. Sample preparation and peel-off adhesion measurement test set-up using cap pull test equipment